

L_1 -Regularized STAP Algorithms With a Generalized Sidelobe Canceler Architecture for Airborne Radar

*Zhaocheng Yang, Rodrigo C. de Lamare, *Senior Member IEEE* and Xiang Li, *Member IEEE*

Abstract—In this paper, we propose novel l_1 -regularized space-time adaptive processing (STAP) algorithms with a generalized sidelobe canceler architecture for airborne radar applications. The proposed methods suppose that a number of samples at the output of the blocking process are not needed for sidelobe canceling, which leads to the sparsity of the STAP filter weight vector. The core idea is to impose a sparse regularization (l_1 -norm type) to the minimum variance criterion. By solving this optimization problem, an l_1 -regularized recursive least squares (l_1 -based RLS) adaptive algorithm is developed. We also discuss the SINR steady-state performance and the penalty parameter setting of the proposed algorithm. To adaptively set the penalty parameter, two switched schemes are proposed for l_1 -based RLS algorithms. The computational complexity analysis shows that the proposed algorithms have the same complexity level as the conventional RLS algorithm ($O((NM)^2)$), where NM is the filter weight vector length), but a far lower complexity level than the loaded sample covariance matrix inversion algorithm ($O((NM)^3)$) and the compressive sensing STAP algorithm ($O((N_s N_d)^3)$), where $N_s N_d > NM$ is the angle-Doppler plane size). The simulation results show that the proposed STAP algorithms converge rapidly and provide a SINR improvement using a small number of snapshots.

Index Terms— l_1 -regularized, Generalized sidelobe canceler architecture, Recursive least squares algorithm, Sparsity, Switched schemes, Space-time adaptive processing, Airborne radar.

I. INTRODUCTION

A requirement of airborne surveillance radar systems is to detect moving targets in a severe and dynamic interference environment which may be composed of clutter and jamming. Space-time adaptive processing (STAP) has been motivated as a key enabling technology for advanced airborne radar applications following the landmark publication by Brennan and Reed [1]. By performing a joint-domain optimization of the spatial and temporal degrees-of-freedom (DOFs), STAP can improve slow-moving target detection through better mainlobe clutter suppression, provide better detection in combined clutter and jamming environments, and offer a significant increase in output signal-to-interference-plus-noise-ratio (SINR), as compared with traditional factored approaches [2], [3], [8]. However, there are many practical limitations preventing the use of the optimum STAP processor, such as a large computational

complexity cost to compute the matrix inversion operation, the requirement of a large number of independent and identically distributed (i.i.d.) training samples to estimate the interference covariance matrix, and the severe non-stationary and heterogeneous interference environment. Thus, much of the work has been focused on addressing the previously mentioned problems in the last decades [4]–[8], [10], [11], [35]. In this paper, we focus on the second problem and devise a STAP technique that improves the convergence speed and tracking performance of existing conventional methods.

More recently, motivated by compressive sensing (CS) techniques used in radar [14]–[16], several authors have considered CS ideas for moving target indication (MTI) and STAP problems [17]–[22]. The core notion in CS is to regularize a linear inverse problem by including prior knowledge that the signal of interest is sparse [21]. A global matched filter (GMF) is applied to the basic STAP problem, which points out that it has the advantage of being able to work on a single snapshot without prior estimation of the interference matrix since the GMF identifies both the targets and a model of the clutter [17]. A novel STAP algorithm based on sparse recovery techniques, called CS-STAP (or SR-STAP sometimes) was presented in [18]–[20]. In their work, the CS-STAP algorithm is divided into two steps: first, the data from much fewer range cells compared with conventional STAP methods is used to estimate the distribution of clutter energy on the spatial-temporal plane by a sparse recovery procedure; second, a novel estimator of the covariance matrix is built based on the result obtained in the first step, and Capon’s optimal filter is constructed with the estimated covariance matrix to suppress clutter. In [22], the angle-Doppler plane is explicitly segmented into the clutter ridge component and a non-clutter-ridge component. Under the assumption of the known clutter ridge in angle-Doppler plane, they impose the sparse regularization to estimate the clutter covariance excluding the clutter ridge. In [21], the authors present a post-processing step after clutter whitening using a standard STAP technique by applying sparse regularization.

The previous works on STAP techniques based on CS technique have focused on the recovery of the clutter power in the angle-Doppler plane, and have not applied the sparse regularization to the STAP filter design. In this paper, we consider a generalized sidelobe canceler (GSC) architecture for STAP in airborne radar, which introduces a blocking process. Since the interference variance has a low rank property [3], [8], we assume that a number of samples at the output of the blocking process are not meaningful for processing,

Z. Yang and X. Li are with Research Institute of Space Electronics, Electronics Science and Engineering School, National University of Defense Technology, Changsha, 410073, China. e-mail: yangzhaocheng@gmail.com, lixiang01@vip.sina.com.

R. C. de Lamare is with Communications Research Group, Department of Electronics, University of York, YO10 5DD, UK. e-mail: rcd1500@ohm.york.ac.uk

which will lead to the sparsity of the filter weight vector. Then, we design the STAP algorithm with another strategy, by imposing the sparse regularization (l_1 -norm type) to the minimum variance (MV) criterion in order to exploit this sparsity feature of the received data and the filter weight vector. This idea is similar to knowledge-aided (KA) STAP [9], [12], [13], which exploits some prior knowledge of the data. With this motivation, the STAP algorithm design becomes a mixed l_1 -norm and l_2 -norm optimization problem, which is currently a vibrant topic [24]–[27]. Sparse least mean-square (LMS) type algorithms and recursive least squares (RLS) type algorithms applied to system identification are studied in [28]–[32], which results in a performance improvement for sparse systems. In this paper, we extend the work presented in [33] to RLS algorithms. We derive the optimal l_1 regularized STAP filter weight vector, propose a modified RLS adaptive algorithm (called l_1 -based RLS) and devise switched schemes to adaptively select the penalty parameter. The simulation results show that this method outperforms the conventional RLS algorithm in terms of SINR steady-state performance and convergence speed, and is much simpler than the CS-STAP [17]–[20].

The main contributions of our paper are listed as follows.

(i) A new l_1 regularized STAP algorithm with GSC architecture for airborne radar is proposed.

(ii) An l_1 -based RLS adaptive algorithm is derived to solve the l_1 regularized GSC-STAP. In order to adaptively set the penalty parameter, two switched schemes are proposed for l_1 -based RLS algorithms.

(iii) The SINR steady-state performance and the penalty parameter setting of the proposed algorithm are discussed, and some useful guidelines are given.

(iv) A study and comparative analysis of our proposed algorithms, (including computation complexity, the SINR steady-state performance and convergence speed) with other STAP algorithms for radar systems is carried out.

This paper is organized as follows. Section II introduces the STAP signal model for airborne radar. In Section III, the full-rank l_1 regularized GSC-STAP algorithm is derived. The SINR steady-state performance and the penalty parameter setting of the proposed algorithm are discussed. Furthermore, the l_1 -based RLS adaptive implementation algorithm and its computational complexity are given. In order to overcome the time-varying interference environment, two switched schemes based on the l_1 -based RLS algorithm are proposed. Some examples illustrating the performance of the proposed l_1 -based RLS algorithms with simulated radar data are shown in Section IV. Finally, the paper ends with some conclusions in Section V.

Notation: In this paper, scalar quantities are denoted with italic typeface. Lowercase boldface quantities denote vectors and uppercase boldface quantities denote matrices. The operations of transposition, complex conjugation, and conjugate transposition are denoted by superscripts T , $*$, and H , respectively. The symbol \otimes represents the Kronecker product. Finally, the symbol $E\{\cdot\}$ denotes the expected value of a random quantity, operator $\Re[\cdot]$ selects the real part of the argument, $\|x\|_1$ and $\|x\|_2$ denote the l_1 -norm and l_2 -norm

operation of x respectively, and $|\cdot|$ denotes the absolute operation.

II. SIGNAL MODEL AND PROBLEM STATEMENT

The system under consideration is a pulsed Doppler radar residing on an airborne platform. The radar antenna is a uniformly linear spaced array (ULA) which consists of M elements. The platform is at altitude h_p and moving with constant velocity v_p . The chosen coordinate system is shown in Fig.1(a). The angle variables ϕ and θ refer to elevation and azimuth. The radar transmits a coherent burst of pulses at a constant pulse repetition frequency (PRF) $f_r = 1/T_r$, where T_r is the pulse repetition interval (PRI). The transmitter carrier frequency is $f_c = c/\lambda_c$, where c is the propagation velocity and λ_c is the wavelength. The coherent processing interval (CPI) length is equal to NT_r . For each PRI, L time samples are collected to cover the range interval. After matched filtering to the radar returns from each pulse, the received data set for one CPI comprises $LN M$ complex baseband samples, which is referred to as the radar datacube shown in Fig.1(b). The data is then processed at one range of interest, which corresponds to a slice of the CPI datacube. The slice is an $M \times N$ matrix which consists of $M \times 1$ spatial snapshots for pulses at the range of interest. It is convenient to stack the matrix columnwise to form the $NM \times 1$ vector $\mathbf{r}[i]$, termed a space-time snapshot, $1 \leq i \leq L$ [1]–[3].

An important task for airborne radar is target detection. Casting the detection problem in the context of binary hypothesis testing, we denote the disturbance only hypothesis by H_0 and the target plus disturbance hypothesis by H_1 .

$$\begin{aligned} H_0 : \mathbf{r} &= \mathbf{r}_u \\ H_1 : \mathbf{r} &= \alpha_t \mathbf{r}_t + \mathbf{r}_u, \end{aligned} \quad (1)$$

where α_t is a complex gain and the $NM \times 1$ space-time steering vector \mathbf{r}_t in the space-time look-direction is defined as [3]

$$\mathbf{r}_t = \mathbf{b}(f_d^t) \otimes \mathbf{a}(f_s^t), \quad (2)$$

where $\mathbf{b}(f_d^t)$ denotes the $N \times 1$ temporal steering vector at the target Doppler frequency f_d^t and $\mathbf{a}(f_s^t)$ denotes the spatial steering vector in the direction provided by the target frequency f_s^t . The steering vectors $\mathbf{a}(f_s^t)$ and $\mathbf{b}(f_d^t)$ are given by

$$\mathbf{a}(f_s^t) = [1, \exp(j2\pi f_s^t), \dots, \exp(j2(M-1)\pi f_s^t)]^T, \quad (3)$$

$$\mathbf{b}(f_d^t) = [1, \exp(j2\pi f_d^t), \dots, \exp(j2(N-1)\pi f_d^t)]^T. \quad (4)$$

The vector \mathbf{r}_u encompasses any undesired interference or noise component of the data including clutter \mathbf{r}_c , jamming \mathbf{r}_j , and thermal noise \mathbf{r}_n . We assume that they are mutually uncorrelated. And the clutter-jammer-noise (for short, calling interference in the following part) covariance matrix \mathbf{R} can be expressed as

$$\mathbf{R} = E\{\mathbf{r}_u \mathbf{r}_u^H\} = \mathbf{R}_c + \mathbf{R}_j + \mathbf{R}_n, \quad (5)$$

where $\mathbf{R}_c = E\{\mathbf{r}_c \mathbf{r}_c^H\}$, $\mathbf{R}_j = E\{\mathbf{r}_j \mathbf{r}_j^H\}$ and $\mathbf{R}_n = E\{\mathbf{r}_n \mathbf{r}_n^H\}$, denote clutter, jammer and thermal noise covariance matrix, respectively.

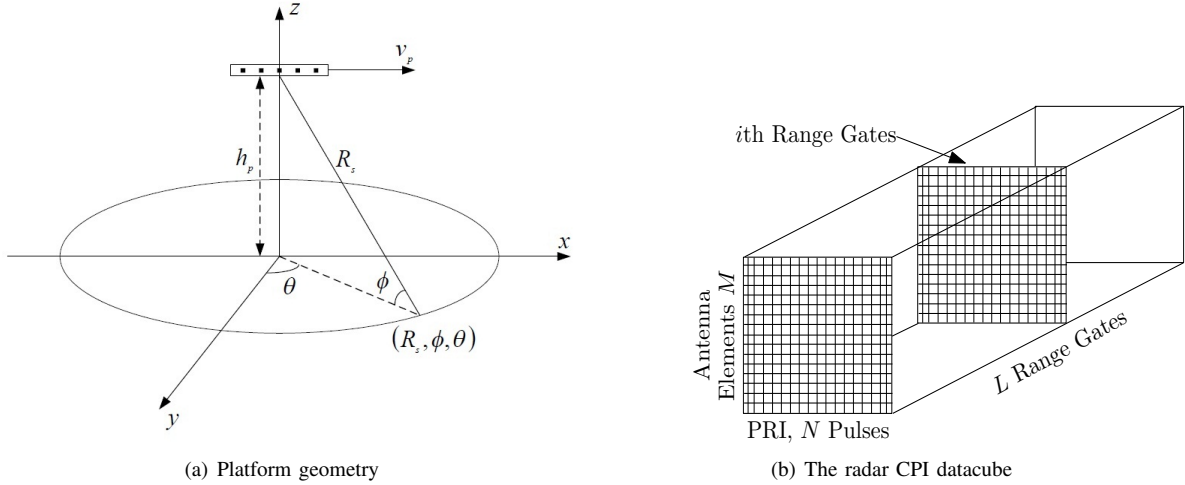


Fig. 1. The radar platform geometry and the radar CPI datacube

The GSC processor results in an unconstrained weight vector and reformulates the STAP detector structure into the form of a standard Wiener filter [10]. The GSC filtering diagram is shown in Fig. 2. Thus we obtain the output of the GSC-STAP as

$$y = d - \mathbf{w}^H \mathbf{x}, \quad (6)$$

where d is the radar mainbeam output which is a scalar, and \mathbf{x} is the $(NM - 1) \times 1$ noise-subspace output data vector, given by

$$d = \mathbf{r}_t^H \mathbf{r}, \quad (7)$$

$$\mathbf{x} = \mathbf{B} \mathbf{r}, \quad (8)$$

where \mathbf{B} is the $(NM - 1) \times NM$ signal blocking matrix, which is composed of any orthogonal basis set for the target steering vector \mathbf{r}_t . Hence, we have

$$\mathbf{B} \mathbf{r}_t = \mathbf{0}. \quad (9)$$

Generally, the blocking matrix \mathbf{B} can be directly obtained by using the singular value decomposition (SVD) and the QR decomposition algorithms [35].

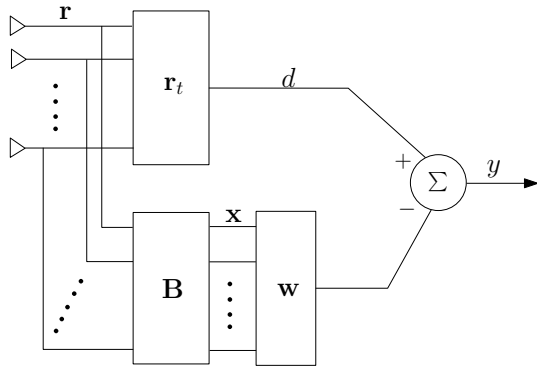


Fig. 2. STAP with GSC architecture for airborne radar

The idea behind the MV approach is to minimize the GSC-STAP output power, which leads to the following power

minimization problem

$$\min_{\mathbf{w}} J(\mathbf{w}) = \min_{\mathbf{w}} E \{ \|\mathbf{y}\|_2^2 \}, \quad (10)$$

where the optimal weight vector is given by

$$\mathbf{w}_{MV} = \mathbf{R}_x^{-1} \mathbf{r}_{xd}, \quad (11)$$

where $\mathbf{R}_x = E\{\mathbf{x}\mathbf{x}^H\}$ denotes the noise-subspace data covariance matrix, and $\mathbf{r}_{xd} = E\{\mathbf{x}d^*\}$ denotes the cross-correlation between the output of the radar mainbeam d and the noise-subspace data vector \mathbf{x} .

Assuming Gaussian-distributed interference, an optimum detection statistic follows from the likelihood ratio test and appears as

$$\Lambda = \frac{|y|^2}{\Psi_0} \underset{H_0}{\overset{H_1}{>}} \eta, \quad (12)$$

where η is the detection threshold, and Ψ_0 is the output-noise power, which is expressed by (13) for the optimal MV filter.

$$\Psi_0 = E\{d^2\} - \mathbf{r}_{xd}^H \mathbf{R}_x^{-1} \mathbf{r}_{xd} = \mathbf{r}_t^H \mathbf{R} \mathbf{r}_t - \mathbf{r}_{xd}^H \mathbf{R}_x^{-1} \mathbf{r}_{xd}, \quad (13)$$

where $\mathbf{R} = E\{\mathbf{r}\mathbf{r}^H\}$, is the input noise-covariance matrix. The performance of (12) is given by

$$P_{fa} = \exp\left(-\frac{\eta^2}{2}\right), \quad (14)$$

$$P_D = \int_{\beta}^{\infty} \mu \exp\left(-\frac{\mu^2 + \rho^2}{2}\right) \mathbf{I}_0(\rho\mu) d\mu, \quad (15)$$

where P_{fa} is the probability of false alarm, P_D is the probability of detection, $\mathbf{I}_0(\cdot)$ is the modified zero-order Bessel function of the first kind and ρ equals the square-root of the peak output SINR, which is expressed by (16) for the optimal MV filter [10], [35]

$$\text{SINR} = \frac{E\{|y_t|^2\}}{\Psi_0} = \frac{\sigma_t^2}{\mathbf{r}_t^H \mathbf{R} \mathbf{r}_t - \mathbf{r}_{xd}^H \mathbf{R}_x^{-1} \mathbf{r}_{xd}}, \quad (16)$$

where $\sigma_t^2 = E\{|\alpha_t|^2\}$, denotes the single-channel, single-pulse signal power. From (15), we can see that P_D depends on both output SINR and the value of P_{fa} . If the value of P_{fa} is specified, P_D is a monotonic function of ρ , that is to say, maximizing SINR is equivalent to maximizing P_D .

III. STAP WITH L_1 -NORM REGULARIZATION

In this section, we detail the design of the proposed l_1 -norm regularized STAP algorithm, discuss the SINR steady-state performance and the penalty parameter setting of the proposed algorithm, and derive the proposed l_1 -based RLS adaptive algorithm. We also propose two switched schemes for the l_1 -based RLS algorithm to adaptively select the penalty parameter and detail their computational complexity.

A. Proposed STAP Algorithm

In STAP applied to radar systems, it is well known that the rank of the clutter subspace is much smaller than the number of system DOFs [3], [8]. In the GSC structure, each row of the blocking matrix may denote a basis of the clutter subspace. Therefore, the clutter subspace can be constructed by only a small number of basis, corresponding to a small number of rows of the blocking matrix, which results in that a number of the samples at the output of the blocking process are not needed for sidelobe canceling. In this case, the signal at the output of the blocking process may have a high degree of sparsity. Since the filtering operation involves a linear mapping between the filter and the received signal, it will lead to the sparsity of the filter coefficients. The conventional STAP algorithms do not exploit this sparsity feature. In this paper, we devise the STAP algorithm by employing an l_1 -regularized condition to the MV criterion. Thus the proposed l_1 -norm regularized STAP can be described as the following optimization problem

$$\min_{\mathbf{w}} J_1(\mathbf{w}), \quad (17)$$

where $J_1(\mathbf{w})$ is the new cost function, defined as

$$J_1(\mathbf{w}) = E \left\{ \|y\|_2^2 \right\} + 2\lambda \|\mathbf{w}\|_1, \quad (18)$$

where λ is a positive scalar which provides a trade-off between sparsity and total squared error. The larger the chosen λ , the more components are shrunk to zero [26]. Now, the question that arises is how to effectively solve the l_1 regularized STAP. In order to solve this problem, we expand the new cost function $J_1(\mathbf{w})$ as

$$J_1(\mathbf{w}) = \mathbf{r}_t^H \mathbf{R} \mathbf{r}_t - (\mathbf{w}^H \mathbf{r}_{xd})^* - \mathbf{w}^H \mathbf{r}_{xd} + \mathbf{w}^H \mathbf{R}_x \mathbf{w} + 2\lambda \|\mathbf{w}\|_1. \quad (19)$$

In order to solve the optimization problem presented in (17), we compute the gradient terms of (19) with respect to \mathbf{w}^* as given by

$$\frac{\partial J_1(\mathbf{w})}{\partial \mathbf{w}^*} = -\mathbf{r}_{xd} + \mathbf{R}_x \mathbf{w} + \lambda \text{sign}(\mathbf{w}), \quad (20)$$

where $\text{sign}(\cdot)$ is a component-wise sign function defined as

$$\text{sign}(x) = \begin{cases} x/|x| & \text{for } x \neq 0 \\ 0 & \text{for } x = 0 \end{cases}. \quad (21)$$

Let us equate (20) to zero, and then we can get

$$\mathbf{w} = \mathbf{R}_x^{-1} [\mathbf{r}_{xd} - \lambda \text{sign}(\mathbf{w})]. \quad (22)$$

This is a sufficient condition of the optimal filter weight vector based on l_1 regularized STAP. Comparing (22) with

the conventional optimal filter weight vector (11), we see that there is an additional term in (22), which is due to the l_1 -norm regularization. However, since the second term on the right-hand side in (22) is a nonlinear function of \mathbf{w} , it is not a solution for the MV criterion. In this paper, under some reasonable assumptions, a solution can be obtained by setting an initial value of \mathbf{w} and running an iterative procedure, which will be shown in the following part.

B. l_1 -Based RLS STAP Algorithm

Generally, in RLS algorithms the noise-subspace data covariance matrix \mathbf{R}_x and the cross-correlation vector \mathbf{r}_{xd} are estimated by the time averaged recursions

$$\mathbf{R}_x[i] = \sum_{n=1}^i \beta^{i-n} \mathbf{x}[n] \mathbf{x}^H[n] = \beta \mathbf{R}_x[i-1] + \mathbf{x}[i] \mathbf{x}^H[i], \quad (23)$$

$$\mathbf{r}_{xd}[i] = \sum_{n=1}^i \beta^{i-n} \mathbf{x}[n] d^*[n] = \beta \mathbf{r}_{xd}[i-1] + \mathbf{x}[i] d^*[i]. \quad (24)$$

For convenience, let

$$\mathbf{g}[i] = \mathbf{r}_{xd}[i] - \lambda \text{sign}(\mathbf{w}[i]). \quad (25)$$

Then, substituting (24) into the above equation, the $\mathbf{g}[i]$ term can be described by a recursive equation, namely

$$\mathbf{g}[i] = \beta \mathbf{g}[i-1] + \mathbf{x}[i] d^*[i] - [\lambda \text{sign}(\mathbf{w}[i]) - \beta \lambda \text{sign}(\mathbf{w}[i-1])]. \quad (26)$$

Assume that the sign of the weight values do not change significantly in a single time step, which is reasonable because we want the instantaneous error of the filter weight vector to change slowly [34], hence, $\mathbf{g}[i]$ can be approximated by

$$\mathbf{g}[i] \approx \beta \mathbf{g}[i-1] + \mathbf{x}[i] d^*[i] + \lambda(\beta - 1) \text{sign}(\mathbf{w}[i-1]). \quad (27)$$

Therefore, the optimal l_1 regularized STAP filter weight vector can be recursively described by

$$\mathbf{w}[i] = \mathbf{R}_x^{-1}[i] \mathbf{g}[i]. \quad (28)$$

Since the matrix inversion $\mathbf{R}_x^{-1}[i]$ is a potentially unstable operation, especially when the matrix is ill-conditioned, in practice, it is replaced by a regularized matrix $(\mathbf{R}_x[i] + \varepsilon \mathbf{I})^{-1}$, where \mathbf{I} is an identity matrix and ε is a small positive number [37].

Denoting $\mathbf{P}[i] = \mathbf{R}_x^{-1}[i]$ and by employing the matrix inversion lemma, we get

$$\mathbf{P}[i] = \frac{1}{\beta} \left[\mathbf{P}[i-1] - \frac{\mathbf{P}[i-1] \mathbf{x}[i] \mathbf{x}^H[i] \mathbf{P}[i-1]}{\beta + \mathbf{x}^H[i] \mathbf{P}[i-1] \mathbf{x}[i]} \right]. \quad (29)$$

Defining the gain vector $\mathbf{k}[i]$ as

$$\mathbf{k}[i] = \frac{\mathbf{P}[i-1] \mathbf{x}[i]}{\beta + \mathbf{x}^H[i] \mathbf{P}[i-1] \mathbf{x}[i]}, \quad (30)$$

and thus we can rewrite $\mathbf{P}[i]$ recursively as

$$\mathbf{P}[i] = \frac{1}{\beta} \left[\mathbf{P}[i-1] - \mathbf{k}[i] \mathbf{x}^H[i] \mathbf{P}[i-1] \right], \quad (31)$$

where $\mathbf{P}[0] = \delta^{-1}\mathbf{I}$, where δ is a small positive constant. Submitting (31), (27) into (28), we obtain the updating l_1 regularized STAP filter weight vector $\mathbf{w}[i]$ as

$$\begin{aligned} \mathbf{w}[i] &= \mathbf{w}[i-1] + \mathbf{k}[i]e^*[i] + \lambda\left(1 - \frac{1}{\beta}\right) \\ &\quad \times [\mathbf{I} - \mathbf{k}[i]\mathbf{x}^H[i]] \mathbf{P}[i-1]\text{sign}(\mathbf{w}[i-1]), \end{aligned} \quad (32)$$

where $e[i] = d[i] - \mathbf{w}^H[i-1]\mathbf{x}[i]$ is the prediction error at time i . Comparing the l_1 -based RLS weight update equation with that of the conventional RLS algorithm, the former has an additional element in the last term of (32), which attracts the weight coefficients to zero for small weight coefficients [28], [30].

The algorithm is summarized in Table I.

TABLE I
THE l_1 -BASED RLS ADAPTIVE ALGORITHM

<p>Initialization: $\mathbf{P}[0] = \delta^{-1}\mathbf{I}$, $\mathbf{w}[0] = \mathbf{0}$, $[\mathbf{U} \ \mathbf{S} \ \mathbf{V}] = \text{svd}(\mathbf{r}_t^T)$, $\mathbf{B} = [\mathbf{V}(:, 2 : N)]^T$</p>
<p>Recursion: For each snapshot $i = 1, \dots, L$ $\mathbf{x}[i] = \mathbf{B}\mathbf{r}[i]$, $d[i] = \mathbf{r}_t^H \mathbf{r}[i]$, $e[i] = d[i] - \mathbf{w}^H[i-1]\mathbf{x}[i]$, $\mathbf{v}[i] = \mathbf{P}[i-1]\mathbf{x}[i]$, $\mathbf{k}[i] = \frac{\mathbf{v}[i]}{\beta + \mathbf{x}^H[i]\mathbf{v}[i]}$, $\mathbf{G}[i] = \mathbf{P}[i-1] - \mathbf{k}[i]\mathbf{v}^H[i]$, $\mathbf{P}[i] = \frac{1}{\beta}\mathbf{G}[i]$, $\mathbf{G}'[i] = \mathbf{G}[i] - \mathbf{P}[i]$, $\mathbf{w}[i] = \mathbf{w}[i-1] + \mathbf{k}[i]e^*[i] + \lambda\mathbf{G}'[i]\text{sign}(\mathbf{w}[i-1])$,</p>
<p>Output: $y[i] = d[i] - \mathbf{w}^H[i]\mathbf{x}[i]$.</p>

C. Setting of the Penalty Parameter

In this section, we will consider the setting of the penalty parameter λ of the proposed STAP algorithm. The SINR steady-state performance of the proposed algorithm will be analyzed and some useful comments of the setting of the penalty parameter λ will be given (the derivation details are seen in Appendix A).

Comment 1: Suppose that \mathbf{w}_{opt} is the conventional optimum GSC-STAP filter weight vector with known interference covariance matrix \mathbf{R} by solving a MV estimation problem described in Section II, $\mathbf{u}_k, k = 1, 2, \dots, NM$ is the eigenvector corresponding to the eigenvalue $\gamma_k, k = 1, 2, \dots, NM$ of the interference covariance matrix, and \mathbf{w}_{l_1} is the steady-state GSC-STAP filter weight vector of the proposed algorithm. Furthermore, assume that $\gamma_1 \geq \gamma_2 \geq \dots \geq \gamma_{NM}$. The SINR steady-state performance of the proposed algorithm SINR_{l_1} is given by [35]

$$\text{SINR}_{l_1} = \frac{\sigma_t^2}{\Psi_{opt} + \Delta\Psi}, \quad (33)$$

where

$$\Psi_{opt} = \tilde{\kappa} = \frac{1}{\mathbf{r}_t^H \mathbf{R}^{-1} \mathbf{r}_t}, \quad (34)$$

$$\Delta\Psi = \lambda^2 \sum_{k=1}^{NM} \frac{1}{\gamma_k} \left(1 - \frac{\tilde{\kappa}}{\gamma_k}\right) \|\text{sign}(\mathbf{w}_{l_1}^H) \mathbf{B}\mathbf{u}_k\|_2^2. \quad (35)$$

The quantities \mathbf{B} and λ are defined in the previous sections. From (33), we know that the SINR steady-state performance will tend to zero with the value of λ approaching infinity, which corresponds to a very bad SINR performance. On the other hand, if the value of λ is close to zero, the steady-state SINR performance will only depend on Ψ_{opt} , which becomes the conventional STAP algorithm resulting in slow SINR convergence speed. By considering a trade-off between the SINR steady-state performance and the SINR convergence speed, the value of λ should be set appropriately. In practical applications, the exact interference covariance matrix can not be obtained and the component Ψ_{opt} will be replaced by $\frac{1}{\mathbf{r}_t^H \hat{\mathbf{R}}^{-1} \mathbf{R} \hat{\mathbf{R}}^{-1} \mathbf{r}_t}$, where $\hat{\mathbf{R}}$ is the estimated interference covariance matrix. When the number of secondary training data is small, the eigenvalue spread of the interference covariance matrix will be large. In this case, the component $\Delta\Psi$ will not always be positive for each iteration. Thus, we may obtain both a better SINR steady-state performance and a faster convergence speed by setting λ properly. In fact, a range of values of λ will lead to some SINR benefits, which will be illustrated by the following simulations.

Comment 2: Assuming that κ_w denotes the number of nonzero coefficients of the steady-state GSC-STAP filter weight vector, σ_n^2 denotes the single-channel, single-pulse thermal noise power, ξ is the interference-to-noise-ratio (INR), χ denotes the rank of the interference covariance matrix, and $\mathbf{u}_k, k = 1, 2, \dots, \chi$ represents the eigenvectors corresponding to large eigenvalues of the interference covariance matrix. For high INR (i.e., the interference is dominant $\xi \gg 1$), the ratio $\frac{\Delta\Psi}{\Psi_{opt}}$, which are defined by (34) and (35) respectively, is a key point to describe the derivation between the SINR steady-state performance of the proposed algorithm and the optimal SINR performance and satisfies

$$\frac{\Delta\Psi}{\Psi_{opt}} \leq (\chi\kappa_w - 1) \frac{\lambda^2}{\sigma_n^4} \sum_{k=1}^{\chi} \mathbf{r}_t^H \mathbf{u}_k \mathbf{u}_k^H \mathbf{r}_t. \quad (36)$$

Offering a trade-off between the SINR steady-state performance and convergence speed, one reasonable setting of the penalty parameter λ is given by

$$\lambda = f\left(\frac{(\chi\kappa_w - 1)}{\sigma_n^4} \sum_{k=1}^{\chi} \mathbf{r}_t^H \mathbf{u}_k \mathbf{u}_k^H \mathbf{r}_t\right), \quad (37)$$

where $f(x)$ is a function of x . One of the simplest functions is the proportional function, which is described as

$$\lambda = \frac{\mu_\lambda \sigma_n^2}{\sqrt{(\chi\kappa_w - 1) \sum_{k=1}^{\chi} \mathbf{r}_t^H \mathbf{u}_k \mathbf{u}_k^H \mathbf{r}_t}}, \quad (38)$$

where μ_λ is the proportionality factor which could be fixed or variant. By inspecting (38), we draw that the setting of the parameter λ should be proportional to the noise power, and be inversely proportional to the rank of the interference covariance matrix. Although we can hardly determine the actual values of κ_w (only know that $\kappa_w < NM$ is a small integer

due to the degree of sparsity of signal) and $\sum_{k=1}^K \mathbf{r}_t^H \mathbf{u}_k \mathbf{u}_k^H \mathbf{r}_t$, (38) is still very useful for setting the penalty parameter λ .

D. Switched l_1 -Based RLS STAP Algorithms

Although some suggestions of setting the penalty parameter λ are given, it is hard to decide the value of λ in a time varying interference environment. In this section, we propose two different switched schemes to adaptively select the proper value of λ .

The first switched scheme (called scheme I) is shown in Fig.3(a). In this proposed scheme, we constrain the penalty parameter λ within a range of appropriate values (the candidates space of the penalty parameter is presented by $\Omega = \{\lambda_k | k = 1, 2, \dots, K\}$). Then, in each iteration, we compute the filter weight vector for each λ_k , $k = 1, 2, \dots, K$ in an independent parallel way just as the approach of the l_1 -based RLS algorithm with fixed penalty parameter. Thus, there will be K independent outputs $\{\mathbf{w}_k[i] | k = 1, \dots, K\}$ from K branches. In particular, we present a method for automatically selecting the filter weight vector from K branches based on the exponentially weighted a posteriori least-squares type cost function, described by

$$C_k[i] = \sum_{n=1}^i \beta^{i-n} \|d[n] - \mathbf{w}_k^H[n] \mathbf{x}[n]\|_2^2, \quad (39)$$

where $k = 1, 2, \dots, K$, β is the forgetting factor, and $\mathbf{w}_k[n]$ is computed by the k th branch using λ_k . $C_k[i]$ also can be represented in a recursive way given by

$$C_k[i] = \beta C_k[i-1] + \|d[i] - \mathbf{w}_k^H[i] \mathbf{x}[i]\|_2^2. \quad (40)$$

Finally, the proposed scheme that chooses the best filter weight vector $\mathbf{w}_{opt}[i]$ for each iteration is given by

$$\mathbf{w}_{opt}[i] = \arg \min_{\mathbf{w}_k[i], k=1,2,\dots,K} C_k[i]. \quad (41)$$

Scheme I is summarized in Table II.

However, scheme I has a much higher computational complexity than the l_1 -based RLS algorithm since it needs to calculate K branches independently in one iteration, especially when K is large. In the following, we propose another switched scheme (called scheme II, as shown in Fig.3(b)), which has a lower computational complexity than scheme I. In this scheme, we also constrain the penalty parameter λ within the candidates space Ω . However, unlike scheme I, there is a feedback from the output of the selected filter weight vector in scheme II, which will be used to calculate the new filter weights for all $\lambda \in \Omega$ and for every snapshot. All the candidate filter weight vectors are computed based on the selected filter weight vector with different values of λ_k , $k = 1, 2, \dots, K$ according to the approach of the l_1 -based RLS algorithm with fixed penalty parameter. Thus, it only needs to calculate the prediction error $e[i] = d[i] - \mathbf{w}_{opt}^H[i-1] \mathbf{x}[i]$ once for all K branches, where \mathbf{w}_{opt} is the selected best filter weight vector obtained from the feedback of the selection box. Similarly, there will be K outputs $\{\mathbf{w}_k[i] | k = 1, \dots, K\}$ from K branches. The proposed scheme II for automatically

TABLE II
THE SWITCHED l_1 -BASED RLS ADAPTIVE ALGORITHM FOR SCHEME I

<p>Initialization: $\mathbf{P}[0] = \delta^{-1} \mathbf{I}$, $\mathbf{w}_k[0] = \mathbf{0}, C_k[0] = 0, k = 1, \dots, K$, $\Omega = \{\lambda_1, \lambda_2, \dots, \lambda_K\}$, $[\mathbf{U} \quad \mathbf{S} \quad \mathbf{V}] = \text{svd}(\mathbf{r}_t^T)$, $\mathbf{B} = [\mathbf{V}(:, 2 : N)]^T$</p>
<p>Recursion: For each snapshot $i = 1, \dots, L$ $\mathbf{x}[i] = \mathbf{B} \mathbf{r}[i]$, $d[i] = \mathbf{r}_t^H \mathbf{r}[i]$, $\mathbf{v}[i] = \mathbf{P}[i-1] \mathbf{x}[i]$, $\mathbf{k}[i] = \frac{\mathbf{v}[i]}{\beta + \mathbf{x}^H[i] \mathbf{v}[i]}$, $\mathbf{G}[i] = \mathbf{P}[i-1] - \mathbf{k}[i] \mathbf{v}^H[i]$, $\mathbf{P}[i] = \frac{1}{\beta} \mathbf{G}[i]$, $\mathbf{G}'[i] = \mathbf{G}[i] - \mathbf{P}[i]$, For $\lambda_k \in \Omega, k = 1, \dots, K$ $e_k[i] = d[i] - \mathbf{w}_k^H[i-1] \mathbf{x}[i]$, $\mathbf{w}_k[i] = \mathbf{w}_k[i-1] + \mathbf{k}[i] e_k^*[i] + \lambda_k \mathbf{G}'[i] \text{sign}(\mathbf{w}_k[i-1])$, $C_k[i] = \beta C_k[i-1] + \ d[i] - \mathbf{w}_k^H[i] \mathbf{x}[i]\ _2^2$, End $\mathbf{w}_{opt} = \arg \min_{\mathbf{w}_k[i], k=1,2,\dots,K} C_k[i]$, Output: $y[i] = d[i] - \mathbf{w}_{opt}^H[i] \mathbf{x}[i]$.</p>

selecting the filter weight vector based on the instantaneous least-squares type cost function $C'_k[i]$, is given by

$$C'_k[i] = \|d[i] - \mathbf{w}_k^H[i] \mathbf{x}[i]\|_2^2. \quad (42)$$

Then we select the best filter weight vector $\mathbf{w}_{opt}[i]$ relying on minimizing the cost function $C'_k[i]$ in each iteration, which is given by

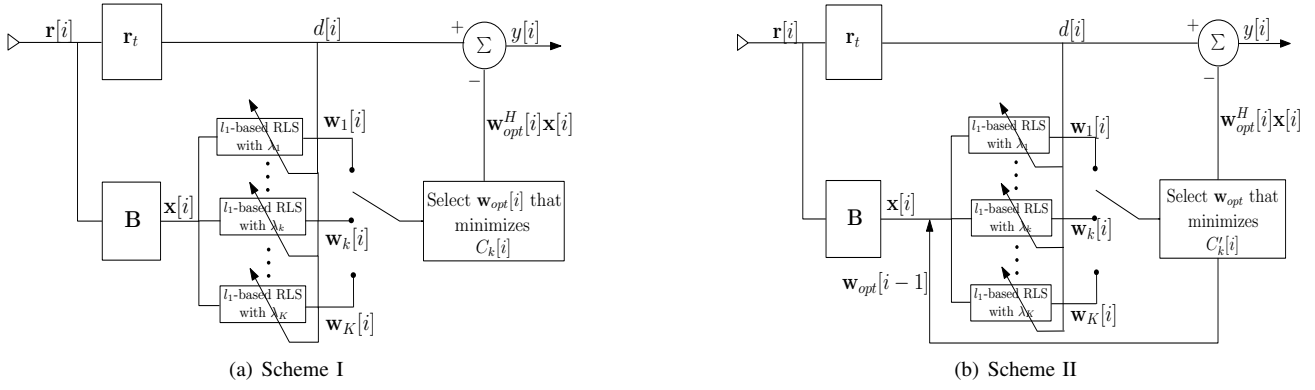
$$\mathbf{w}_{opt}[i] = \arg \min_{\mathbf{w}_k[i], k=1,2,\dots,K} C'_k[i], \quad (43)$$

where $\mathbf{w}_k[i]$ is computed using λ_k and the selected filter weight vector $\mathbf{w}_{opt}[i-1]$ by the k th branch. Scheme II is summarized in Table III.

Seen from the previous discussions, two aspects should be noted. The first one is that one of the important differences of both proposed schemes lies in the fact that scheme II has a lower computation complexity, but more complex structure since it requires the feedback from the selection box, compared with scheme I. That is to say scheme I is more convenient for realizing with nowadays parallel processors. Therefore, both scheme I and scheme II have their own advantages to adaptively select a proper value of λ and which one is better relies on the requirements of practical applications. The second one is that it requires some prior knowledge to decide the range of λ in both proposed schemes. A drawback of the proposed schemes is that it may not guarantee to select an optimal λ , if the range of λ could not be determined properly. The development of alternative and effective methods for automatic adjustment of λ remains an interesting open area for investigation.

E. Complexity Analysis

We detail the computational complexity per snapshot of the conventional loaded sample matrix inversion (LSMI) algorithm, the conventional RLS algorithm, the proposed l_1 -based

Fig. 3. Switched l_1 -based RLS STAP schemes.TABLE IV
COMPUTATIONAL COMPLEXITY FOR PER SNAPSHOT

Algorithm	Additions	Multiplications
LSMI	$O((NM-1)^3) + 3(NM)^2 - 4NM + 1$	$O((NM-1)^3) + 4(NM)^2 - 4NM + 1$
RLS	$3(NM)^2 - 3NM$	$4(NM)^2 - 2NM - 1$
l_1 -based RLS	$5(NM)^2 - 7NM + 2$	$5(NM)^2 - 3NM - 1$
Switched l_1 -based RLS I	$(4+K)(NM)^2 + (K-7)NM - K + 3$	$(4+K)(NM)^2 + (2K-4)NM - K + 1$
Switched l_1 -based RLS II	$5(NM)^2 + (2K-8)NM - 2K + 3$	$5(NM)^2 + (2K-4)NM - K$

TABLE III
THE SWITCHED l_1 -BASED RLS ADAPTIVE ALGORITHM FOR SCHEME II

<p>Initialization: $\mathbf{P}[0] = \delta^{-1}\mathbf{I}$, $\mathbf{w}_{opt}[0] = \mathbf{0}$, $C'_k[0] = 0, k = 1, \dots, K$, $\Omega = \{\lambda_1, \lambda_2, \dots, \lambda_K\}$, $[\mathbf{U} \ \mathbf{S} \ \mathbf{V}] = \text{svd}(\mathbf{r}_t^T)$, $\mathbf{B} = [\mathbf{V}(:, 2:N)]^T$</p>
<p>Recursion: For each snapshot $i = 1, \dots, L$ $\mathbf{x}[i] = \mathbf{B}\mathbf{r}[i]$, $d[i] = \mathbf{r}_t^H \mathbf{r}[i]$, $\mathbf{v}[i] = \mathbf{P}[i-1]\mathbf{x}[i]$, $\mathbf{k}[i] = \frac{\mathbf{v}[i]}{\beta + \mathbf{x}^H[i]\mathbf{v}[i]}$, $\mathbf{G}[i] = \mathbf{P}[i-1] - \mathbf{k}[i]\mathbf{v}^H[i]$, $\mathbf{P}[i] = \frac{1}{\beta}\mathbf{G}[i]$, $\mathbf{G}'[i] = \mathbf{G}[i] - \mathbf{P}[i]$, $e[i] = d[i] - \mathbf{w}_{opt}^H[i-1]\mathbf{x}[i]$, $\mathbf{w}'[i] = \mathbf{w}_{opt}[i-1] + \mathbf{k}[i]e^*[i]$, For $\lambda_k \in \Omega, k = 1, \dots, K$ $\mathbf{w}_k[i] = \mathbf{w}'[i] + \lambda_k \mathbf{G}'[i] \text{sign}(\mathbf{w}_{opt}[i-1])$, $C'_k[i] = \ d[i] - \mathbf{w}_k^H[i]\mathbf{x}[i]\ _2^2$, End $\mathbf{w}_{opt}[i] = \arg \min_{\mathbf{w}_k[i], k=1,2,\dots,K} C'_k[i]$, Output: $y[i] = d[i] - \mathbf{w}_{opt}^H[i]\mathbf{x}[i]$.</p>

RLS algorithm and the switched l_1 -based RLS algorithms as shown in Table IV. The computational requirements are described in terms of the number of complex arithmetic operations, namely, additions and multiplications. From the table, we note that the complexity of the proposed l_1 -based RLS algorithm is at the same level as the conventional RLS algorithm ($O((NM)^2)$), but much lower than that of the conventional LSMI algorithm ($O((NM)^3)$). The computa-

tional complexity of the proposed switched l_1 -based RLS schemes depends on the candidate size K of λ . However, the computational complexity of scheme II is lower than that of scheme I, and is only a little higher than that of the l_1 -based RLS algorithm with fixed penalty parameter (in fact only $2(NM)^2 + (2K-5)NM - 2K + 2$ additions and $(NM)^2 + 2(K-1)NM - K + 1$ multiplications). As for scheme I, it is more convenient for realizing with nowadays parallel processors because of no feedback requirement.

IV. SIMULATION RESULTS

In this section, we assess the proposed l_1 -based RLS adaptive algorithms using simulated radar data. The parameters of the simulated radar platform are shown in Table V. In the following examples, we assume the forgetting factor is $\beta = 0.9998$, use zero vectors for the initialization of filter weight vectors and $\delta^{-1}\mathbf{I}$ for the initialization of the inverse of the interference covariance matrix for the proposed algorithms and the RLS algorithm, where δ is a small constant. The blocking matrix \mathbf{B} is computed by the SVD operation on a matrix composed by the space-time steering vectors. All presented results are averaged over 100 independent Monte Carlo runs.

A. Setting of the Penalty Parameter

In our first experiment, we will examine the SINR performance of our proposed l_1 -based RLS algorithm with different values of the l_1 -norm penalty parameter λ . We assume that the number of antenna elements is $M = 8$, the number of pulses in one CPI is $N = 8$, and the penalty parameter λ is set to $\lambda = 0, 1, 5, 10, 20, 50, 100$, respectively. The evaluation of the SINR performance against snapshots with different values of λ is shown in Fig.4, where the algorithm is simulated over

TABLE V
RADAR SYSTEM PARAMETERS

Parameter	Value
Antenna array	sideway-looking array
Antenna array spacing	$\lambda/2$
Carrier frequency	450MHz
Transmit pattern	Uniform
Mainbeam azimuth	0°
PRF	300Hz
Platform velocity	50m/s
Platform height	9000 m
Thermal noise power	10^{-2}
Clutter-to-noise-ratio (CNR)	30dB
Jammer-to-noise-ratio (JNR)	30dB
Jammer azimuth	60° and -45°
Signal-to-noise-ratio (SNR)	0dB
Target Doppler	100Hz
Target azimuth	0°
Antenna elements number	8
Pulse number in one CPI	8

$L = 500$ snapshots. The result indicates that: (i) the value of λ is crucial to the SINR performance, and there is a range of values of λ for the proposed algorithm, which can improve the SINR steady-state performance and convergence speed, e.g. $1 \leq \lambda \leq 50$; (ii) the SINR steady-state performance is even worse than that of the conventional RLS algorithm when λ is too large since the STAP filter weights will be shrunk to zero; (iii) the SINR steady-state performance and convergence speed will not improve much when λ is too small. In this case, it has nearly the same SINR performance as the conventional RLS algorithm.

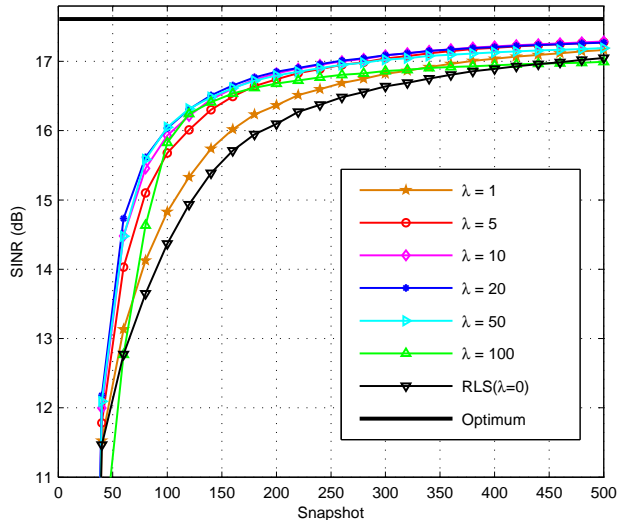


Fig. 4. SINR performance against snapshot with $\lambda = 0, 1, 5, 10, 20, 50, 100$, $\delta = 8 \times 10^{-2}$ and $\sigma_n^2 = 10^{-2}$.

In the next experiment, we evaluate the relationship between the penalty parameter λ and the thermal noise power σ_n^2 . We assume that the parameters of the simulated radar platform are the same as those in the first experiment except for the thermal noise power, which is $\sigma_n^2 = 10^{-1}$. From the first example, we

know that the SINR performance and convergence speed are both satisfactory when $\lambda = 20$. In order to have a further evaluation of the setting of λ , we consider two cases, which are $\lambda = 20$ and $\lambda = 200$. The result is shown in Fig.5. It can be seen from this figure that the setting of the parameter λ should be proportional to the thermal noise power, otherwise it will result in a worse SINR performance.

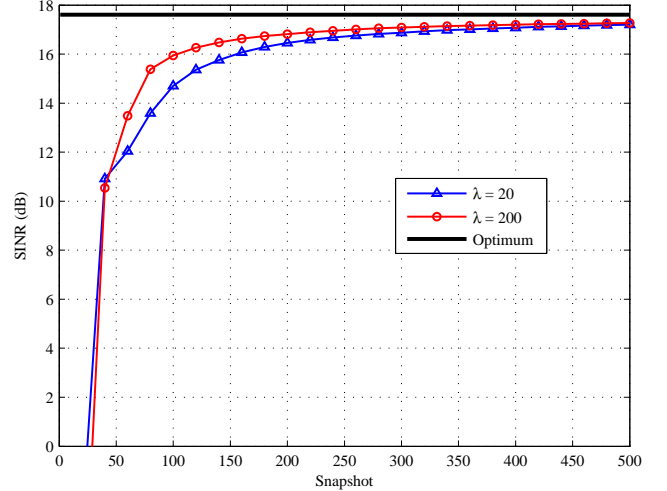


Fig. 5. SINR performance against snapshot with $L = 500$ snapshots, $\lambda = 20, 200$, $\delta = 2 \times 10^{-1}$ and $\sigma_n^2 = 10^{-1}$.

In this experiment, we focus on the SINR performance of the switched l_1 -based RLS STAP algorithms. It is seen from the second experiment that the SINR performance depends on the value of λ , which is sensitive to the thermal noise power. In practice, the thermal noise power is time varying and its covariance is also time-varying. And we do not know the exact value of the thermal noise power covariance, but know a range of that. Thus, according to this, we could choose a number of reasonable values of λ , which is set to $\lambda = 0, 5, 10, 20, 30, 40, 50$ in this experiment. Assume that the thermal noise power covariance is $\sigma_n^2 = 2.25 \times 10^{-2}$, which is different from the above two experiments. In Fig.6, we see that the SINR performance of the proposed switched l_1 -based RLS algorithms is always the best, compared with others with fixed value of λ . And we know that it is no longer the best choice to set the $\lambda = 10$ or $\lambda = 20$.

Moreover, compared with the RLS algorithm, the curves in Fig.6 show an excellent steady-state SINR performance and a faster SINR convergence speed versus snapshot by the proposed algorithms (not only the switched l_1 -based RLS algorithms, but also the l_1 -based RLS algorithm with fixed values of λ). In the following experiments, in order to have a clear presentation of the simulation results, we will not draw all the curves (but only one of them) computed by the l_1 -based RLS algorithm with fixed values of λ in each figure. This is also because it has been shown that the proposed switched l_1 -based RLS algorithms provide better performance than the l_1 -based RLS algorithm with fixed values of λ in Fig.6.

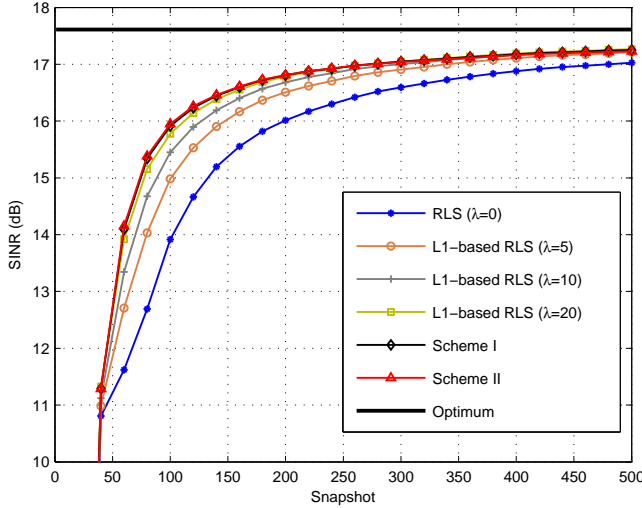


Fig. 6. SINR performance against snapshot with $L = 500$ snapshots, $\delta = 8 \times 10^{-2}$ and $\sigma_n^2 = 2.25 \times 10^{-2}$. The candidates of switched l_1 -based RLS schemes are $\lambda = 0, 5, 10, 20, 30, 40, 50$.

B. Comparison With the RLS Algorithm

In the fourth experiment, as shown in Fig.7, we present the P_D versus SNR performance for our proposed algorithms and the RLS algorithm using 100 snapshots as the training data. The false alarm rate P_{fa} is set to 10^{-6} and we suppose the target is injected in the boresight (0°) with Doppler frequency 100Hz. The other parameters are the same as the third experiment. The figure illustrates that the proposed algorithms provide suboptimal detection performance using small support data, but remarkably, obtain much higher detection rate than the conventional RLS algorithm at an SNR level from 0dB to 11dB. Note that the detection performance of the proposed switched l_1 -based RLS algorithms are better than that of the l_1 -based RLS algorithm with fixed values of λ .

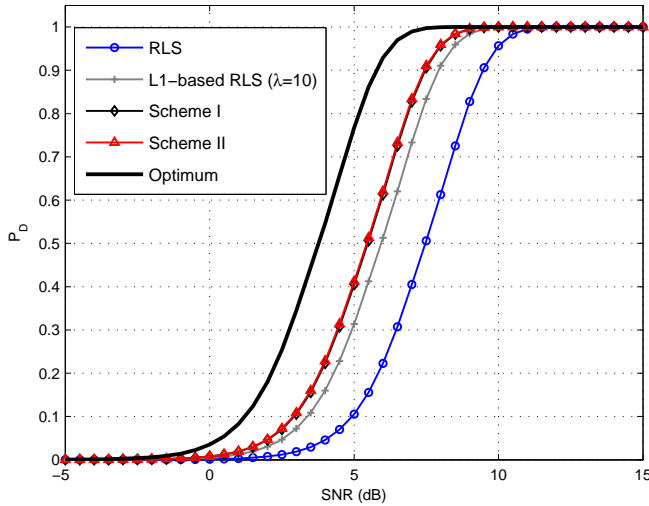


Fig. 7. Probability of detection performance versus SNR with $L = 100$ snapshots, $P_{fa} = 10^{-6}$, $\delta = 8 \times 10^{-2}$ and $\sigma_n^2 = 2.25 \times 10^{-2}$. The candidate space of switched l_1 -based RLS schemes is $\Omega = 0, 5, 10, 20, 30, 40, 50$.

We then evaluate the SINR performance against the target Doppler frequency at the main beam look angle for the RLS algorithm and our proposed algorithms, which is illustrated in Fig.8. The potential Doppler frequency space from -100 Hz to 100 Hz is examined and $L = 100$ snapshots are used to train the filter and the other parameters are the same as the third experiment. The plots show that the proposed algorithms provide a suboptimum SINR performance, but they outperform the conventional RLS algorithm in most of the Doppler bins, and form a deeper null to cancel the main beam clutter than the conventional RLS algorithm. The same conclusion can be obtained from the plot showing the SINR against Doppler frequency of the proposed switched l_1 -based RLS algorithms, which are better than that of the l_1 -based RLS algorithm with fixed values of λ .

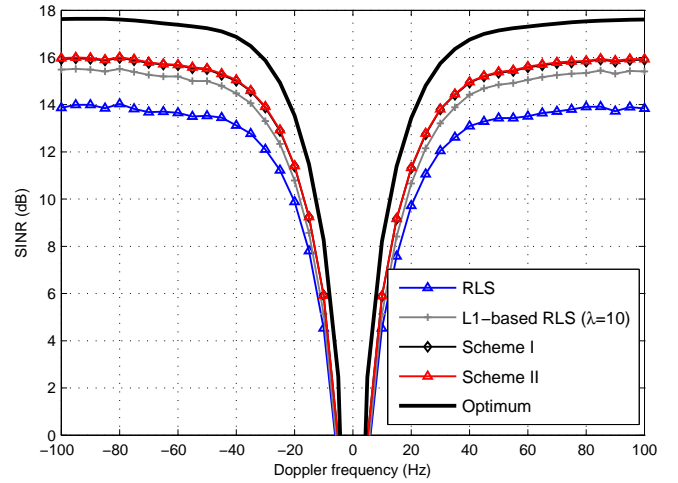


Fig. 8. SINR performance against Doppler frequency with $L = 100$ snapshots, Doppler frequency space from -100 to 100 Hz, $\delta = 8 \times 10^{-2}$ and $\sigma_n^2 = 2.25 \times 10^{-2}$. The candidate space of switched l_1 -based RLS schemes is $\Omega = 0, 5, 10, 20, 30, 40, 50$.

C. Comparison With Other Algorithms

In this section, we will evaluate the SINR performance against the number of snapshots L of our proposed algorithms with the recently developed CS-STAP algorithm, the conventional LSMI algorithm, and the conventional RLS algorithm in another scenario, which is adopted in [20]. The basic idea of the CS-STAP is firstly to estimate the clutter spectrum α by solving the following minimization problem

$$\alpha = \arg \min \|\alpha\|_1 \quad \text{s.t.} \min \|\mathbf{r} - \mathbf{H}\alpha\|_2 \leq \varepsilon, \quad (44)$$

where ε is the noise allowance, and \mathbf{H} is a $MN \times N_s N_d$ (the space angle and Doppler frequency axes are discretized into $N_s = \rho_s M, N_d = \rho_d N, \rho_s, \rho_d > 1$ grids in the angle-Doppler domain to obtain the clutter spectrum with high resolution), defined as following

$$\mathbf{H} = [\mathbf{h}(f_{d,1}, f_{s,1}), \dots, \mathbf{h}(f_{d,1}, f_{s,N_s}), \dots, \mathbf{h}(f_{d,N_d}, f_{s,1}), \dots, \mathbf{h}(f_{d,N_d}, f_{s,N_s})], \quad (45)$$

where $\mathbf{h}(f_{d,i}, f_{s,i})$ is the $NM \times 1$ space-time steering vector with the normalized Doppler frequency $f_{d,i}$ and the normalized spatial frequency $f_{s,i}$. The above l_1 norm minimization can be carried out via convex optimization tools [20], [38]. Finally, the space-time adaptive filter is computed by the conventional method and the clutter covariance matrix estimation is given by

$$\hat{\mathbf{R}}_{sr} = \sum_{i=1}^{N_s N_d} |\bar{\alpha}_i|^2 \mathbf{h}(f_{d,i}, f_{s,i}) \mathbf{h}(f_{d,i}, f_{s,i})^H + \delta_{sr} \mathbf{I}, \quad (46)$$

where δ_{sr} is a small loading factor, and $\bar{\alpha}_i$ denotes the i th element of the averaged clutter spectrum $\bar{\alpha}$, which can be calculated by multiple snapshots, given by

$$|\bar{\alpha}_i|^2 = \frac{1}{L} \sum_{n=1}^L |\hat{\alpha}_i[n]|^2. \quad (47)$$

Let us now consider two scenarios: (i) case I, one jammer with azimuth 30° ; (ii) case II, one jammer with azimuth 10° . All of them assume that the azimuthal extent of the clutter distribution is between $30^\circ \sim 50^\circ$, and the other parameters of the simulated radar platform are the same as those in Table V. Moreover, we set the number of snapshots to $L = 100$. In the CS-STAP algorithm, consider two different sizes of the angle-Doppler plane, one is discretized into $N_s = 2M + 1$ by $N_d = 2N + 1$, and the other is $N_s = 4M + 1$ by $N_d = 4N + 1$. The clutter covariance matrix loading factor is $\delta_{sr} = 10^{-3}$ for case I, and $\delta_{sr} = 10^{-4}$ for case II. The noise allowances for both cases are set to $\varepsilon = 10^{-4}$. In the LSMI algorithm, the diagonal loading factor is $\delta_{smi} = 3 \times 10^{-1}$. In the RLS algorithm and the proposed algorithms, $\beta = 0.9998$ for both cases, $\delta = 0.15$ for case I and $\delta = 0.1$ for case II. In the switched l_1 -based RLS algorithms, the λ space is $\Omega = [0, 5, 10, 20, 30, 40, 50]$.

As shown in Fig.9(a), the plots depict that the SINR performance and the SINR convergence speed of our proposed algorithms outperform the conventional LSMI algorithm, and the conventional RLS algorithm. Although the SINR convergence speed of CS-STAP algorithm is faster than that of our proposed algorithms, the SINR steady-state performance of our proposed algorithms is better than that when the number of snapshots is larger than 20 for $N_s = 2M + 1$ by $N_d = 2N + 1$, and 50 for $N_s = 4M + 1$ by $N_d = 4N + 1$. Note that a better SINR steady-state performance and a faster SINR convergence speed of the CS-STAP algorithm are obtained by increasing a much larger size of angle-Doppler plane, which will lead to a much higher computational complexity. From Fig.9(b), we see that the SINR steady-state performance and convergence speed of the CS-STAP algorithm are seriously reduced when the jammer locates near the target, but those of our proposed algorithms almost keep the same SINR level and perform better than the other algorithms. This is because the estimation of the clutter spectrum via convex optimization in the CS-STAP algorithm is not sufficiently accurate in this situation. Furthermore, it is also shown that the proposed switched l_1 -based algorithms could adaptively select the best λ and achieve a better SINR performance than the l_1 -based RLS algorithm with fixed values of λ .

The computational complexity of the CS-STAP algorithm is very high. The clutter spectrum recovery (requiring computation $O((N_s N_d)^3)$) is the additional computation compared with the LSMI, whose computational complexity is $O((NM)^3)$. To have an assessment of the computational complexity of all algorithms, we count the flops required by the analyzed algorithms of this experiment using the Lightspeed Matlab toolbox [40] in Fig.10. The computational complexity curves show that the CS-STAP algorithm has a much higher complexity than the other algorithms, which makes it hard to implement in practice. The complexity of our proposed algorithms is a little higher than that of the conventional RLS algorithm, but much lower than that of the LSMI algorithm and the CS-STAP algorithm. Furthermore, the CS-STAP algorithm needs to determine the appropriate size of the angle-Doppler plane, which has a serious effect on the SINR performance. The larger the size of angle-Doppler plane, much higher the computational complexity required. Therefore, our proposed algorithms have a relative low complexity and are more practical.

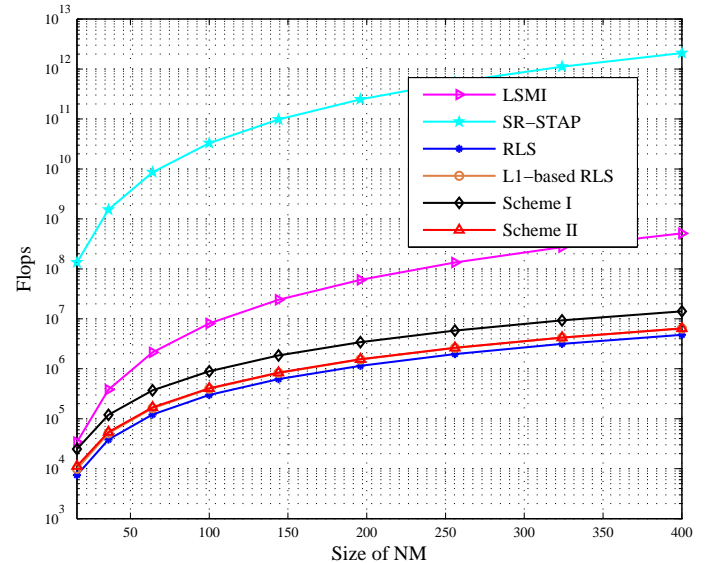


Fig. 10. The computational complexity of all algorithms against the size of system DOFs per snapshot with the size of λ space $K = 7$. In the CS-STAP algorithm, the angle-Doppler plane is discretized into two different sizes, one $N_s = 2M + 1$ by $N_d = 2N + 1$, and the other $N_s = 4M + 1$ by $N_d = 4N + 1$.

V. CONCLUSIONS

In this paper, we have proposed novel l_1 -regularized STAP algorithms with GSC architecture for airborne radar systems. This proposed method exploits the sparsity of the received data and the STAP filter weights, and imposes a sparse regularization (l_1 -norm) to the MV criterion. In order to solve this mixed l_1 -norm and l_2 -norm problem, we have developed an l_1 -based RLS adaptive algorithm. The computational complexity of the proposed l_1 -based RLS algorithm is a little higher than that of the conventional RLS algorithm. However, it has much lower computational complexity than the LSMI algorithm and the CS-STAP algorithm. To overcome the

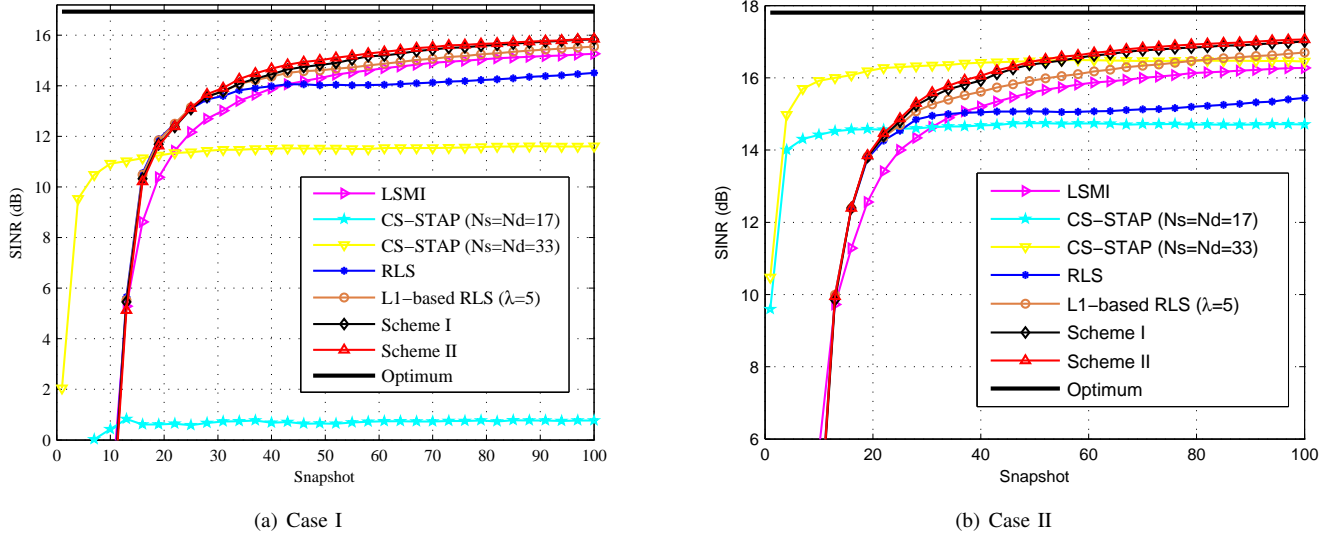


Fig. 9. The SINR performance against snapshot with $L = 100$ snapshots. Consider two scenarios: (i) case I, one jammer with azimuth 30° ; (ii) case II, one jammer with azimuth 10° . Assume that the azimuthal extent of the clutter distribution is between $30^\circ \sim 50^\circ$. In the CS-STAP algorithm, the angle-Doppler plane is discretized into two different sizes, one $N_s = 2M + 1$ by $N_d = 2N + 1$, and the other $N_s = 4M + 1$ by $N_d = 4N + 1$.

time-varying environment, two switched schemes have been proposed to adaptively select the proper penalty parameter for l_1 -based RLS algorithms. The simulation results have shown that the proposed algorithms outperform the conventional RLS algorithm in terms of the SINR steady-state performance and convergence speed, and have a much lower complexity than the CS-STAP and the LSMI algorithms.

APPENDIX A PROOF OF SECTION III-C

Proof: The output SINR of proposed STAP strategy SINR_{l_1} is

$$\text{SINR}_{l_1} = E \left[\frac{\sigma_t^2}{\|\mathbf{r}_t^H \mathbf{r} - \mathbf{w}_{l_1}^H \mathbf{B} \mathbf{r}\|_2^2} \right], \quad (48)$$

where \mathbf{w}_{l_1} is the filter weight vector computed by the proposed STAP strategy and the denominator can be rewritten as

$$\begin{aligned} \Psi &= \|\mathbf{r}_t^H \mathbf{r} - \mathbf{w}_{l_1}^H \mathbf{B} \mathbf{r}\|_2^2 \\ &= \mathbf{r}_t^H \mathbf{R} \mathbf{r}_t - 2\Re \{ \mathbf{w}_{l_1}^H \mathbf{B} \mathbf{R} \mathbf{r}_t \} \\ &\quad + \mathbf{w}_{l_1}^H \mathbf{B} \mathbf{R} \mathbf{B}^H \mathbf{w}_{l_1}. \end{aligned} \quad (49)$$

Substituting (22) into (16), (49) can be obtained as

$$\Psi = \Psi_{opt} + \Delta\Psi, \quad (50)$$

where Ψ_{opt} denotes the noise output power of the conventional STAP strategy, and $\Delta\Psi$ is the deviation between the proposed STAP strategy and conventional STAP strategy, respectively given by

$$\Psi_{opt} = \mathbf{r}_t^H \mathbf{R} \mathbf{r}_t - \mathbf{r}_t^H \mathbf{R} \mathbf{B}^H (\mathbf{B} \mathbf{R} \mathbf{B}^H)^{-1} \mathbf{B} \mathbf{R} \mathbf{r}_t, \quad (51)$$

$$\Delta\Psi = \lambda^2 \text{sign}(\mathbf{w}_{l_1}^H) (\mathbf{B} \mathbf{R} \mathbf{B}^H)^{-1} \text{sign}(\mathbf{w}_{l_1}). \quad (52)$$

Usually, using the eigenvalue decomposition, the interference covariance matrix \mathbf{R} can be presented as [36]

$$\mathbf{R} = \sum_{k=1}^{NM} \gamma_k \mathbf{u}_k \mathbf{u}_k^H, \quad (53)$$

where $\gamma_1 \geq \gamma_2 \geq \dots \geq \gamma_{NM}$ is the eigenvalues of the interference covariance matrix, \mathbf{u}_k is eigenvector corresponding to γ_k , $k = 1, 2, \dots, NM$. In a data adaptive mode of operation, the steady-state performance of the GSC STAP processor and the direct-form STAP processor based on linearly constrained minimum variance (LCMV) criterion are identical [35]. The optimal weight vector of the direct-form STAP processor can be described by

$$\mathbf{w}_{dfp} = \left(\mathbf{r}_t - \sum_{k=1}^{NM} \left(1 - \frac{\tilde{\kappa}}{\gamma_k} \right) \mathbf{u}_k \mathbf{u}_k^H \mathbf{r}_t \right), \quad (54)$$

where

$$\begin{aligned} \frac{1}{\tilde{\kappa}} &= \mathbf{r}_t^H \mathbf{R}^{-1} \mathbf{r}_t \\ &= \sum_{k=1}^{NM} \frac{1}{\gamma_k} \mathbf{r}_t^H \mathbf{u}_k \mathbf{u}_k^H \mathbf{r}_t. \end{aligned} \quad (55)$$

The total optimal weight vector of the GSC STAP processor can be obtained from (11), which is

$$\mathbf{w}_{gsc} = \left(\mathbf{r}_t - \mathbf{B}^H (\mathbf{B} \mathbf{R} \mathbf{B}^H)^{-1} \mathbf{B} \mathbf{R} \mathbf{r}_t \right). \quad (56)$$

Comparing (56) with (55), we have

$$\mathbf{B}^H (\mathbf{B} \mathbf{R} \mathbf{B}^H)^{-1} \mathbf{B} \mathbf{R} = \sum_{k=1}^{NM} \left(1 - \frac{\tilde{\kappa}}{\gamma_k} \right) \mathbf{u}_k \mathbf{u}_k^H, \quad (57)$$

With some matrix transformations, we can obtain $(\mathbf{BRB}^H)^{-1}$ from the above equation, described as

$$(\mathbf{BRB}^H)^{-1} = \sum_{k=1}^{NM} \frac{1}{\gamma_k} \left(1 - \frac{\tilde{\kappa}}{\gamma_k}\right) \mathbf{B} \mathbf{u}_k \mathbf{u}_k^H \mathbf{B}^H. \quad (58)$$

In the above equation, we use the fact that $\mathbf{BB}^H = \mathbf{I}$ [39]. Therefore, inserting (53), (57) and (58) in (51) and (52), we get

$$\begin{aligned} \Psi_{opt} &= \sum_{k=1}^{NM} \gamma_k \mathbf{r}_t^H \mathbf{u}_k \mathbf{u}_k^H \left[\mathbf{I} - \sum_{k=1}^{NM} \left(1 - \frac{\tilde{\kappa}}{\gamma_k}\right) \mathbf{u}_k \mathbf{u}_k^H \right] \mathbf{r}_t \\ &= \sum_{k=1}^{NM} \tilde{\kappa} \mathbf{r}_t^H \mathbf{u}_k \mathbf{u}_k^H \mathbf{r}_t \\ &= \tilde{\kappa} \sum_{k=1}^{NM} \|\mathbf{r}_t^H \mathbf{u}_k\|_2^2 \\ &= \tilde{\kappa}, \end{aligned} \quad (59)$$

$$\begin{aligned} \Delta \Psi &= \lambda^2 \sum_{k=1}^{NM} \frac{1}{\gamma_k} \left(1 - \frac{\tilde{\kappa}}{\gamma_k}\right) \text{sign}(\mathbf{w}_{l_1}^H) \mathbf{B} \mathbf{u}_k \mathbf{u}_k^H \mathbf{B}^H \text{sign}(\mathbf{w}_{l_1}) \\ &= \lambda^2 \sum_{k=1}^{NM} \frac{1}{\gamma_k} \left(1 - \frac{\tilde{\kappa}}{\gamma_k}\right) \|\text{sign}(\mathbf{w}_{l_1}^H) \mathbf{B} \mathbf{u}_k\|_2^2. \end{aligned} \quad (60)$$

In (59), we use the normalization condition $\mathbf{r}_t^H \mathbf{r}_t = 1$. Let σ_n^2 denotes the single-channel, single-pulse noise power, ξ denotes the INR, and χ denotes the rank of the interference covariance matrix (i.e. the number of large eigenvalues). For high INR (i.e., the interference is dominant $\xi \gg 1$), then $\gamma_{min} = \sigma_n^2$, and $\frac{1}{\tilde{\kappa}}$ in (55) can be simplified as

$$\begin{aligned} \frac{1}{\tilde{\kappa}} &\approx \frac{1}{\gamma_{min}} \sum_{k=\chi+1}^{NM} \mathbf{r}_t^H \mathbf{u}_k \mathbf{u}_k^H \mathbf{r}_t \\ &= \frac{1}{\gamma_{min}} \left[1 - \sum_{k=1}^{\chi} \mathbf{r}_t^H \mathbf{u}_k \mathbf{u}_k^H \mathbf{r}_t \right] \\ &= \frac{1}{\sigma_n^2} \left[1 - \sum_{k=1}^{\chi} \mathbf{r}_t^H \mathbf{u}_k \mathbf{u}_k^H \mathbf{r}_t \right]. \end{aligned} \quad (61)$$

Thus, the ratio $\frac{\Delta \Psi}{\Psi_{opt}}$, defined by (59) and (60), is computed by

$$\begin{aligned} \frac{\Delta \Psi}{\Psi_{opt}} &= \lambda^2 \sum_{k=1}^{NM} \frac{1}{\gamma_k} \left(\frac{1}{\tilde{\kappa}} - \frac{1}{\gamma_k} \right) \|\text{sign}(\mathbf{w}_{l_1}^H) \mathbf{B} \mathbf{u}_k\|_2^2 \\ &\approx \frac{\lambda^2}{\gamma_{min}} \left(\frac{1}{\tilde{\kappa}} - \frac{1}{\gamma_{min}} \right) \left[1 - \sum_{k=1}^{\chi} \|\text{sign}(\mathbf{w}_{l_1}^H) \mathbf{B} \mathbf{u}_k\|_2^2 \right] \\ &= \frac{\lambda^2}{\sigma_n^4} \sum_{k=1}^{\chi} \mathbf{r}_t^H \mathbf{u}_k \mathbf{u}_k^H \mathbf{r}_t \\ &\quad \times \left[\sum_{k=1}^{\chi} \|\text{sign}(\mathbf{w}_{l_1}^H) \mathbf{B} \mathbf{u}_k\|_2^2 - 1 \right]. \end{aligned} \quad (62)$$

Using the Cauchy-Schwarz inequality to (62), we obtain

$$\begin{aligned} \frac{\Delta \Psi}{\Psi_{opt}} &\leq \frac{\lambda^2}{\sigma_n^4} \sum_{k=1}^{\chi} \mathbf{r}_t^H \mathbf{u}_k \mathbf{u}_k^H \mathbf{r}_t \\ &\quad \times \left[\sum_{k=1}^{\chi} \|\text{sign}(\mathbf{w}_{l_1}^H) \mathbf{B}\|_2^2 \|\mathbf{u}_k\|_2^2 - 1 \right] \\ &= (\chi \kappa_{\mathbf{w}} - 1) \frac{\lambda^2}{\sigma_n^4} \sum_{k=1}^{\chi} \mathbf{r}_t^H \mathbf{u}_k \mathbf{u}_k^H \mathbf{r}_t, \end{aligned} \quad (63)$$

where $\kappa_{\mathbf{w}}$ denotes the number of nonzero coefficients of the steady-state GSC-STAP filter weight vector.

REFERENCES

- [1] L. E. Brennan and L. S. Reed, "Theory of adaptive radar," *IEEE Transactions on Aerospace and Electronic Systems*, vol.9, no.2, pp.237-252, 1973.
- [2] J. Ward, "Space-time adaptive processing for airborne radar," *Technical Report 1015*, MIT Lincoln laboratory, Lexington, MA, vol. Dec. 1994.
- [3] W. L. Melvin, "A STAP overview," *IEEE Aes. Ele. Sys. Mag.*, vol.19, no.1, pp.19-35, 2004.
- [4] A. M. Haimovich and Y. Bar-Ness, "An eigenanalysis interference canceler," *IEEE Transactions on Signal Processing*, vol.39, no.1, pp.76-84, 1991.
- [5] H. Wang and L. Cai, "On adaptive spartial-temporal processing for airborne surveillance radar systems," *IEEE Transactions on Aerospace and Electronic Systems*, vol.30, no.3, pp.660-670, 1994.
- [6] R. C. de Lamare and R. Sampaio-Neto, "Reduced-rank adaptive filtering based on joint and iterative optimization of adaptive filters," *IEEE Signal Processing Letters*, vol.14, no.12, pp.980-983, 2007.
- [7] R. C. de Lamare and R. Sampaio-Neto, "Adaptive reduced-rank processing based on joint and iterative interpolation, decimation, and filtering," *IEEE Transactions on Signal Processing*, vol.57, no.7, pp.2503-2514, 2009.
- [8] R. Fa, R. C. de Lamare and L. Wang, "Reduced-rank STAP schemes for airborne radar based on swithced joint interpolation, decimation and filtering algorithm," *IEEE Trans. Sig. Proc.*, vol.58, no.8, pp.4182-4194, 2010.
- [9] R. Fa and R. C. de Lamare, "Knowledge-aided reduced-rank STAP for MIMO radar based on based on joint iterative constrained optimization of adaptive filters with multiple constraints," *IEEE Int. Conf. Acoust. Speech and Signal Processing*, pp.2762-2765, 2010.
- [10] J. S. Goldstein, I. S. Reed and P. A. Zulch, "Multistage Partially Adaptive STAP CFAR Detection Algorithm," *IEEE Transactions on Aerospace and Electronic Systems*, vol.35, no.2, pp.645-661, 1999.
- [11] D. A. Pados and G. N. Karystinos, "An iterative algorithm for the computation of the MVDR filter," *IEEE Transactions on Signal Processing*, vol.49, no.2, pp.290-300, Feb. 2001.
- [12] J. R. Guerci and E. J. Baranoski, "Knowledge-Aided adaptive radar at DARPA: an overview," *IEEE Signal Processing Magazine*, vol.23, no.1, pp.41-50, 2006.
- [13] W. L. Mevin and G. A. Showman, "An approach to Knowledge-Aided covariance estimation," *IEEE Transactions on Aerospace and Electronic Systems*, vol.42, no.3, pp.1021-1042, Jul. 2006.
- [14] M. A. Herman and T. Strohmer, "High-resolution radar via compressed sensing," *IEEE Transactions on Signal Processing*, vol.57, no.6, pp.2275-2284, Jun. 2009.
- [15] K. R. Varshney, M. Cetin, J. W. Fisher and A. S. Willsky, "Sparse representation in structured dictionaries with application to synthetic aperture radar," *IEEE Transactions on Signal Processing*, vol.56, no.8, pp.3548-3561, Aug. 2008.
- [16] M. T. Alonso, P. Lopez-Dekker and J. J. Mallorqui, "A novel strategy for radar imaging based on compressive sensing," *IEEE Transactions on Geoscience and Remote Sensing*, vol.48, no.12, pp.4285-4295, Dec. 2010.
- [17] S. Maria and J. J. Fuchs, "Application of the global matched filter to STAP data an efficient algorithmic approach," *IEEE Int. Conf. Acoust. Speech and Signal Processing*, pp. 14-19, 2006.
- [18] K. Sun, H. Zhang, G. Li, H. Meng and X. Wang, "A novel STAP algorithm using sparse recovery technique", *IGARSS*, pp.336-339, 2009.

- [19] H. Zhang, G. Li, and H. Meng, "A class of novel STAP algorithms using sparse recovery technique", 2009[Online]. Available: <http://arxiv.org/abs/0904.1313>.
- [20] K. Sun, H. Zhang, G. Li, H. Meng and X. Wang, "Airborne radar STAP using sparse recovery of clutter spectrum", 2010[Online]. Available: <http://arxiv.org/abs/1008.4185>.
- [21] J. T. Parker and L. C. Potter, "A Bayesian perspective on sparse regularization for STAP post-processing", *IEEE Radar Conference*, pp.1471-1475, May 2010.
- [22] I. W. Selesnick, S. U. Pillai, K. Y. Li and B. Himed, "Angle-Doppler processing using sparse regularization", *IEEE Int. Conf. Acoust. Speech and Signal Processing*, pp.2750-2753, 2010.
- [23] R. Fa, R. C. de Lamare and V. H. Nascimento, "Knowledge-Aided STAP Algorithm Using Convex Combination of Inverse Covariance Matrices for Heterogeneous Clutter", *Proc. IEEE Int. Conf. Acoust., Speech and Signal Processing*, pp.2742-2745, Sep. 2010.
- [24] M. Elad, "Why simple shrinkage is still relevant for redundant representations," *IEEE Transactions on Information Theory*, vol. 52, no. 12, pp. 5559-5569, Dec. 2006.
- [25] M. Zibulevsky and M. Elad, "L1-L2 optimization in signal and image processing," *IEEE Sig. Proc. Mag.*, vol. 27, no. 3, pp. 76-88, May 2010.
- [26] D. Angelosante, J. A. Bazerque and G. B. Giannakis, "Online adaptive estimation of sparse signals: where RLS meets the l_1 -norm," *IEEE Trans. Sig. Proc.*, vol. 58, no. 7, pp. 3436-3446, 2010.
- [27] J. Friedman, T. Hastie and R. Tibshirani, "Regularization paths for generalized linear models via coordinate descent," *Journal of Statistical Software*, vol. 33, no. 1, pp. 1-22, Jan. 2010.
- [28] Y. Chen and Y. Gu and A. Hero, "Sparse LMS for system identification," *IEEE Int. Conf. Acoust. Speech and Signal Processing*, pp. 3125-3128, Apr. 2009.
- [29] Y. Chen and Y. Gu and A. Hero, "Regularized least-mean-square algorithms," 2009[Online]. Available: <http://arxiv.org/abs/1012.5066>.
- [30] J. Jin, Y. Gu and S. Mei, "A stochastic gradient approach on compressive sensing signal reconstruction based on adaptive filtering framework," *IEEE Journal of Selected Topics in Signal Processing*, vol. 4, no. 2, pp. 409-420, Apr. 2010.
- [31] E. M. Eksioğlu, "RLS adaptive filtering with sparsity regularization," *10th Int. Conf. Information Science, Signal Processing and their Applications*, pp. 550-553, 2010.
- [32] D. Angelosante and G. B. Giannakis, "RLS-weighted Lasso for adaptive estimation of sparse signals," *IEEE Int. Conf. Acoust. Speech and Signal Processing*, pp. 3245-3248, 2009.
- [33] Z. Yang, R. C. de Lamare and X. Li, " L_1 regularized STAP algorithm with a generalized sidelobe canceler architecture for airborne radar," *Proc. IEEE Workshop on Statistical Signal Processing*, pp.329-332, June 2011.
- [34] S. Haykin, *Adaptive filter theory (4th Edition)*. Englewood Cliffs, NJ: Prentice-Hall, 2001.
- [35] J. S. Goldstein and I. S. Reed, "Theory of partially adaptive radar," *IEEE Transactions on Aerospace and Electronic Systems*, vol.33, no.4, pp.1309-1325, Oct. 1997.
- [36] J. R. Guerci, *Space-time adaptive processing for radar*. Artech House, 2003.
- [37] P. S. D. Diniz, *Adaptive filtering: algorithms and practical implementation (second edition)*. Kluwer Academic Publishers, 2002.
- [38] <http://www.stanford.edu/~boyd/cvx>.
- [39] H. L. Van Trees, *Optimal array processing, part IV of detection, estimation and modulation theory*. New York: John Wiley & Sons, Inc., 2002.
- [40] <http://research.microsoft.com/en-us/um/people/minka/software/lightspeed/>.



Zhaocheng Yang received the B.E. degree from Beijing Institute of Technology, Beijing, P.R. China, in 2007. He pursued the M.Sc. degree in National University of Defense Technology, Changsha, China from September 2007 to December 2008. From March 2009 he is a PhD student in electrical engineering from National University of Defense Technology. Since November 2010 to now, he is a visiting scholar at University of York, York, U.K..

His research interests lie in the area of statistical signal processing, including array signal processing, adaptive signal processing and its applications to radar systems.



Rodrigo C. de Lamare received the electronic engineering degree from the Federal University of Rio de Janeiro (UFRJ), Brazil, in 1998 and the M.Sc. and Ph.D. degrees in electrical engineering from the Pontifical Catholic University of Rio de Janeiro (PUCRIO), Brazil, in 2001 and 2004, respectively.

Since January 2006, he has been with the Communications Research Group, Department of Electronics, University of York, York, U.K., where he is currently a lecturer in communications engineering.

His research interests lie in communications and signal processing, areas in which he has published about 220 papers in refereed journals and conferences.

Dr. de Lamare is a senior member of the IEEE and an Associate Editor for the *EURASIP Journal on Wireless Communications and Networking*. He has served as the General Chair of the 7th IEEE International Symposium on Wireless Communications Systems, held in York, U.K., in September 2010.



Xiang Li received the B.E. degree from Xidian University, Xian, P.R. China, in 1989 and the M.Sc. and Ph.D. degrees in electrical engineering from National University of Defense Technology, Changsha, China, in 1995 and 1998, respectively.

He is currently a Professor with the Electronics Science and Engineering School, National University of Defense Technology, Changsha, China. His research interests include radar signal processing, radar imaging and automatic target recognition.